Heliyon 9 (2023) e19540

Contents lists available at ScienceDirect

Heliyon

journal homepage: www.cell.com/heliyon

FOXG1 regulates the proliferation and apoptosis of human lung cancer cells

Yan Chen [a,1], Yuqing Wang [a,1], Caiting Yang [a,1], Xiaoting Zhang [b], Yongxin Liu [a], Genyuan Pu [a], Huijie Jiang [a], Yun Pan [b], Zhenjin Li [b,**], Mingming Lai [a,*]

[a] Dali University, Dali, 671000, China
[b] Dali University Affiliated Hospital, Dali, 671000, China

A B S T R A C T

FOXG1, a transcriptional factor belonging to the Forkhead Box (Fox) superfamily, is highly expressed in the brain tissue during brain development and plays an important role in cellular proliferation. Recently, FOXG1 was reported to play important roles in oncogenesis, wherein its abnormal expression regulates tumor cell proliferation. However, the expression and role of FOXG1 in lung cancer remain largely unknown. This study investigated the clinical significance, expression, and role of FOXG1 in lung cancer. We found that FOXG1 was highly expressed in lung cancer tissues. MTT, CCK-8 and colony formation assays showed that FOXG1 overexpression could enhance the proliferation of A549 lung cancer cells. Flow cytometry analysis revealed that FOXG1 promoted the cell cycle and suppressed cell apoptosis. Additionally, the expression levels of PTEN, phosphorylated AKT, mTOR, p53, and Bax were significantly altered in response to changes in FOXG1 expression, indicating that FOXG1 regulated the PI3K pathway. Furthermore, in the xenograft mouse model, the upregulated FOXG1 expression strongly promoted tumor growth. In conclusion, these results suggested that FOXG1 was a critical regulator of the proliferation of lung cancer cells and enhanced tumor growth *in vivo*.

1. Introduction

Lung cancer is the second most commonly diagnosed cancer and the leading cause of cancer-related deaths worldwide, and it causes more than 600,000 deaths annually. The 5-year survival of patients with lung cancer since diagnosis is only 10%–20% in most countries [1]. Although screening for lung cancer can partly reduce the disease burden, the unique biological characteristics of this tumor largely limit therapeutic efficacy. Therefore, gaining an in-depth understanding of the molecular mechanisms underlying lung cancer progression is necessary for identifying novel molecular targets and improving the therapeutic effects of lung cancer.

Forkhead box G1 (FOXG1), also known as brain factor-1, belongs to the winged-helix forkhead family of transcription factors and acts mainly as a transcriptional repressor by binding to the DNA [2]. FOXG1 is highly expressed in the brain tissues and is required for telencephalon development [3–5]. Defective expression of FOXG1 in humans can lead to Rett syndrome and other forms of mental retardation [6,7]. FOXG1 expression is strongly correlated with the proliferation capacity of cells. The sustained high expression of FOXG1 is important for maintaining the number of neural progenitor cells [8]. Recently, more studies have focused on the role of FOXG1 in tumorigenesis. Abnormalities in FOXG1 expression were observed in many types of tumors, such as glioblastoma, breast carcinoma, ovarian carcinoma, hepatoblastoma, and nasopharyngeal carcinoma [9–13]. In most cancers, FOXG1 has an upregulated expression, promoting cell proliferation. In glioblastoma and ovarian carcinoma, FOXG1 could increase cell proliferation through

* Corresponding author.
** Corresponding author.
E-mail addresses: lzj8zsy@163.com (Z. Li), mingminglai1985@aliyun.com (M. Lai).
[1] These authors contributed equally to this work.

https://doi.org/10.1016/j.heliyon.2023.e19540
Received 31 January 2023; Received in revised form 14 August 2023; Accepted 25 August 2023
Available online 26 August 2023

interfering with TGF-β signaling [14]. It has also been reported that FOXG1 was involved in negative regulation of cell apoptosis, but the mechanism was not clear [13]. Nevertheless, in breast cancer, FOXG1 has shown low expression, which is also correlated with a poor prognosis. However, information on the role of FOXG1 in lung cancer is scarce, necessitating an in-depth exploration.

FOXG1 expression is upregulated in lung cancer cell lines, especially in small cell lung cancer (SCLC) cell lines, which suggests that FOXG1 might serve as a potential therapeutic target for lung cancer [15]. In the present study, we analyzed the expression and clinical significance of FOXG1 in lung cancer, after which we investigated the role of FOXG1 in the proliferation of lung cancer cells. We also determined the underlying mechanisms.

2. Materials and methods

2.1. Bioinformatics analysis

The clinicopathological and FOXG1 expression profiles of patients with non-SCLC (small cell lung cancer) were obtained from The Cancer Genome Atlas (TCGA) database. Samples with incomplete or missing clinicopathological and prognostic follow-up data were excluded. The Perl software program and "limma" of R package V3.5.3 in R software were used to collect and transform FOXG1 expression data. The "survival" R package V3.5.3 was used to plot the overall survival curves for patients with non-SCLC. The FOXG1 expression profiles in SCLC were obtained from the Oncomine database. The critical criteria were set as $P < 0.05$, fold change 1.5, and gene rank = All.

2.2. Clinical samples

Thirty-two patients who had a diagnosis of SCLC in the Affiliated Hospital of Dali University from 2018 to 2019 were included in this study. All enrolled patients received no chemotherapy, radiotherapy, or targeted therapy before surgery, and had no medical history of other malignant tumors. All resected tissues were preserved in paraffin. This work was approved by the Ethics Committee of Dali University (approval no.: MECDU-201711-27), and all patients provided written informed consent.

2.3. Cell culture

Cell lines A549 and HEK-293T were obtained from the National Collection of Authenticated Cell Cultures (Shanghai, China). These cells were cultured in Dulbecco's modified Eagle's medium (Meilunbio, Dalian, China) supplemented with 10% fetal bovine serum (Meilunbio, Dalian, China), 100 μg/mL streptomycin, and 100 U/mL penicillin (Meilunbio, Dalian, China) at 37 °C in a 5% CO_2 humidified incubator. Mycoplasma testing was performed using a mycoplasma detection kit (Beyotime, Shanghai, China).

2.4. Establishment of stable cell lines

cDNA encoding human FOXG1 was amplified by polymerase chain reaction (PCR) and subcloned into the lentiviral vector pWPXLd-IRES Puro, which was kindly provided by Dr. Tao Yang (Xuzhou Medical University, China). The viral plasmids pSPAX2, pMD2.G, and pWPXLd-IRES Puro were transfected into HEK-293T cells at a ratio of 3:1:4 using lipo8000TM (Beyotime, Shanghai, China). Furthermore, 72 h after transfection, the cell supernatant was collected, and the virus was purified. The purified virus was used for infecting A549 cells. After 72 h, the infected A549 cells were cultured in a complete medium supplemented with 2.0 μg/mL purinomycin to establish stable cell lines.

2.5. Quantitative real-time PCR

Total RNA was extracted from cells using the Total RNA Isolation Kit (Vazyme, Nanjing, China). Then, the extracted total RNA was used as the template for the synthesis of cDNA with the HiScript 1st Strand cDNA Synthesis Kit (Vazyme, Nanjing, China). Quantitative real-time PCR (qPCR) was performed on StepOnePlus™ Real-Time PCR System, using ChamQ SYBR qPCR Master Mix (Vazyme, Nanjing, China). GAPDH was used as the endogenous control. The relative mRNA expression level was determined according to the $2^{-\Delta\Delta Ct}$ model. The primers used in the study are as follows: GAPDH-F, ACACCCACTCCTCCACCTTT; GAPDH-R, TAGCCAAATTCGTTGTCATACC; FOXG1-F, CAATGACTTCGCAGAGCAGC; FOXG1-R, GGGTTGGAAGAAGACCCCTG.

2.6. MTT assay

A549 cells were seeded in 96-well plates with a density of 1.5×10^3 cells per well. Cell proliferation ability was measured at 24, 48, and 72 h using the MTT kit (Meilunbio, Dalian, China). 10 μL MTT was added to each well and incubate for 4 h 100 μL Formazan was then added to dissolve the precipitate. The absorbance was read at 570 nm using a microplate reader (Epoch 2, Agilent Technologies, USA).

2.7. Cell Counting Kit-8 assay

A549 cells were seeded into 96-well plates, at a density of 4×10^3 cells per well. Cell viability was measured at 24, 48, and 72 h

using the CCK-8 kit (Dojindo, Japan). All operations were performed according to the manufacturer's protocol.

2.8. Colony formation assay

A549 cells were seeded into 6-well plates at a density of 0.7×10^3 cells per well. After 7 days of incubation, the cells were washed with phosphate-buffered saline (PBS) and stained with crystal violet. Visible cell colonies were observed and imaged using an inverted microscope (IX53, OLYMPUS, Japan).

2.9. Flow cytometry analysis

Flow cytometry analysis was performed on a FACS Calibur (BD Biosciences, San Jose, CA, USA). Cell cycle analysis was performed according to the manufacturer's instructions of the Cell Cycle and Apoptosis Analysis Kit (Biosharp, Hefei, China). A549 cells were harvested and rinsed with PBS. After fixing with 70% ethanol at 4 °C overnight, the cells were stained with 1 × propidium iodide staining solution at 37 °C for 30 min away from light, and then, the cells were used to analyze for their cell cycle.

Cell apoptosis analysis was performed using the PE Annexin V Apoptosis Detection Kit I (BD Biosciences, San Jose, CA, USA). A549 cells were harvested and rinsed with PBS and then resuspended in 1 × binding buffer at a density of 1×10^6 cells/mL. In each group, 100 μL of cell suspension was mixed with 5 μL of PE Annexin V and 5 μL of 7-AAD and incubated at room temperature (25 °C) for 15 min in the dark. Then, 400 μL of 1 × binding buffer was added to each tube to analyze cell apoptosis.

2.10. Immunohistochemistry assay

The assays were performed as described previously [16]. After antigen retrieval with 0.01 M citrate buffer, the slices were blocked with goat serum at room temperature for 20 min and then incubated with the primary antibody (*anti*-FOXG1 antibody, 1:800, AB-18259, Abcam) at 4 °C overnight. The slices were developed using the SABC (Rabbit IgG)-POD Kit (SA2002, BOSTER, Wuhan, China). The nuclei were stained with hematoxylin. The images were obtained using the Olympus BX51 laser scanning confocal microscope (Tokyo, Japan).

2.11. Western blotting

Western blot analysis was performed as described previously [17]. Radioimmunoprecipitation assay lysis buffer was used to extract the total protein from the cells. Protein concentrations were quantified using the BCA Protein Quantification Kit (TIANGEN, Beijing, China). Subsequently, the protein extracts were separated using sodium dodecyl sulfate–polyacrylamide gel electrophoresis and then transferred onto polyvinylidene difluoride membranes (Millipore, Boston, MA, USA). The membranes were then incubated with the primary antibody (*anti*-FOXG1 antibody, 1:1,000, AB-18259, Abcam; *anti*-p21WAF1/CIP1 antibody, 1:1,000, A1438, ABclonal; anti–proliferating cell nuclear antigen (PCNA) antibody, 1:1,000, CB104, ABclonal; anti-PI3K antibody, 1:1,000, #4249, Cell Signaling; *anti*-Akt1 antibody, 1:1,000, #2938, Cell Signaling; *anti*-pAkt (Thr308) antibody, 1:1,000, #13038, Cell Signaling; *anti*-pAkt (Thr473) antibody, 1:1,000, #31957, Cell Signaling; *anti*-Phospho-mTOR (Ser2448) antibody, 1:1,000, HA600094, Huaan Bio; *anti*-p53 antibody, 1:1,000, #2527, Cell Signaling; *anti*-PTEN antibody, 1:1,000, #9188 fg, Cell Signaling; *anti*-Bax antibody, 1:1,000, #2774, Cell Signaling; *anti*-GAPDH antibody, 1:10,000, AC002, ABclonal) at 4 °C overnight. After washing three times with Tris-buffered saline with Tween 20 (TBST), the membranes were incubated with horseradish peroxidase (HRP)–coupled secondary antibody (HRP goat antirabbit IgG H&L, 1:10,000, AS014; ABclonal; HRP goat antimouse IgG H&L, 1:10,000, AS003, ABclonal) at room temperature for 1 h. The membranes were washed with TBST again. Finally, the protein bands were developed with an ECL western blotting substrate reaction kit (Solarbio, Beijing, China) and detected using an automatic chemiluminescence imaging system (Tanon, China).

2.12. Xenograft model

A549-NC and A549-FOXG1 cells in the logarithmic growth phase were resuspended in PBS and adjusted to a cell density of 1×10^6 cells/mL. The cells (1×10^6) were injected subcutaneously into the right flank of BALB/c nude mice. The tumor size was measured after 2 weeks when visible tumor nodules appeared at the inoculation sites. Tumor diameters were measured using digital calipers, and tumor volume (in mm^3) was calculated using the following formula: Tumor volume = $(\text{width})^2 \times \text{length}/2$. The maximum diameter of the tumor nodules was less than 15 mm. At the end of the experiments, the mice were euthanized through CO_2 asphyxiation.

2.13. Statistical analysis

Statistical analyses were conducted, and graphics were generated using GraphPad Prism 7.00 software and R software (version 3.5.3). Data were presented as mean ± standard deviation. Log-rank test was used to calculate survival rates. Student's t-test was used for analyzing the differences between the two groups. One-way analysis of variance with Tukey's post hoc test was used for analyzing the differences among multiple groups. $P < 0.05$ indicated statistical significance.

3. Results

3.1. FOXG1 expression was upregulated in lung cancer

We evaluated FOXG1 transcriptional levels in multiple lung cancer studies from TCGA and Oncomine databases. The results showed that FOXG1 expression was upregulated in patients with lung adenocarcinoma (LUAD) and lung squamous cell carcinoma (LUSC) when compared with that in healthy individuals (Fig. 1A and B). Kaplan-Meier survival analysis revealed that the higher expression level of FOXG1 was related to the poor prognosis of patients with LUAD in terms of overall survival (Fig. 1C and D). Because of the lack of small cell lung cancer (SCLC) data in the TCGA database, we analyzed FOXG1 expression in SCLC from the Oncomine database. Statistical analysis showed that FOXG1 was significantly overexpressed in SCLC (Fig. 1E). We also collected 32 samples from patients with SCLC and measured FOXG1 expression. Immunohistochemistry analysis showed that positive staining of FOXG1 was substantially increased in SCLC samples, and the positive straining was concentrated mainly at the nuclei (Fig. 1F and G). These data suggest that FOXG1 expression was elevated in clinical SCLC samples.

3.2. FOXG1 promotes the proliferation of lung cancer cells

To further investigate the role of FOXG1 in lung cancer, we examined FOXG1 expression in three lung cancer cell lines. Consistent with previous study [15], FOXG1 had the lower expression in the human LUAD cell line A549 when compared with that in the human SCLC cell lines NCI–H446 and NCI–H1688 (Fig. 2A and B, and Fig. S1). Therefore, we constructed A549 cell lines stably overexpressing FOXG1 (A549-FOXG1) using the lentivirus system and negative control (A549-NC). Fig. 2C shows effective transfection in A549 cells. As shown in Fig. 2D, FOXG1 was effectively overexpressed in A549 cells (Fig. S2). Next, we performed MTT, CCK8 and colony formation assays to investigate the possible role of FOXG1 in lung cancer cell proliferation. As shown in Fig. 2E–G, cell proliferation was significantly enhanced in FOXG1-overexpressed cells compared with that in control cells ($P < 0.01$). The expression of proliferating cell nuclear antigen (PCNA), a marker of cell proliferation, was evaluated in A549-FOXG1 cells in comparison with A549-NC cells (Fig. 3C, and Fig. S3). The results indicated that FOXG1 overexpression promoted a higher proliferation rate in lung cancer cells.

3.3. Effects of FOXG1 on cell cycle and apoptosis

We speculated whether the increased cell proliferation induced by FOXG1 was the result of cell cycle or apoptosis regulation. As shown in Fig. 3, FOXG1 overexpression led to a significant decrease in the percentage of G0/G1 phase cells and an accompanied increase in the percentage of G2/M phases cells when compared with the control ($P < 0.01$) (Fig. 3 A, B). Consistently, the expression of p21WAF1/CIP1, a cyclin-dependent kinases inhibitor which mediates cell cycle arrest in G1 phase, was significantly decreased in FOXG1-transfected cells when compared with control cells ($P < 0.01$) (Fig. 3C, D, and Fig. S3). These data indicated that cell cycle progression was induced during FOXG1 overexpression.

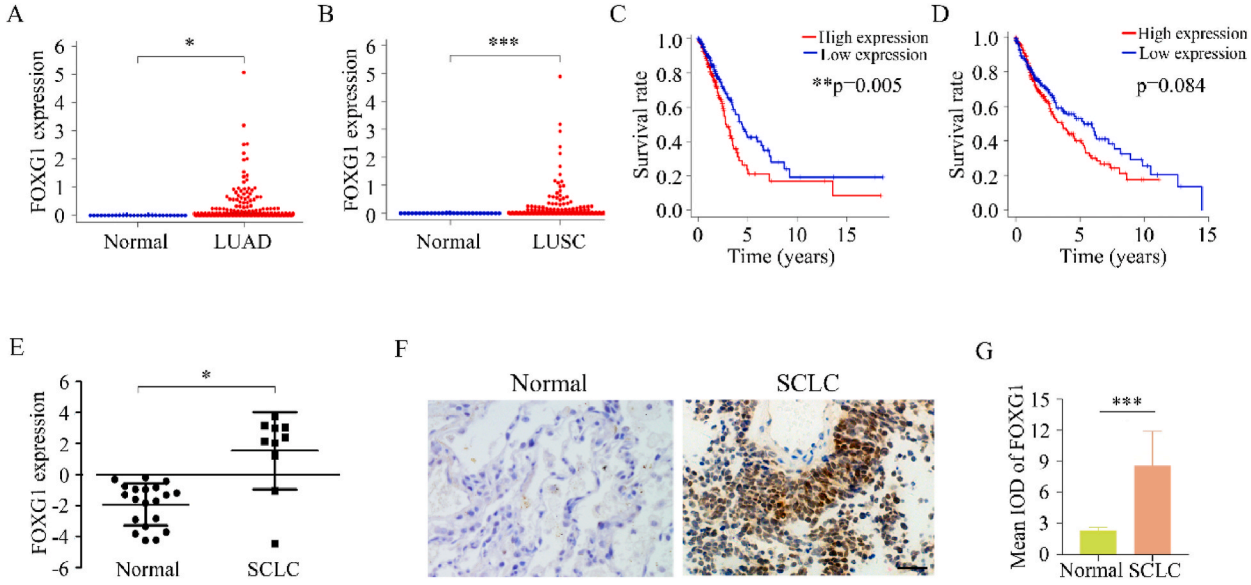

Fig. 1. Upregulated FOXG1 expression in lung cancer. **A** and **B** FOXG1 expression analysis in LUAD and LUSC tissues when compared with normal tissues using data from the TCGA database. **C** and **D** Survival analysis in patients with LUAD or LUSC according to relative FOXG1 expression levels. **E** FOXG1 expression analysis in SCLC from the Oncomine database. **F** and **G** Immunohistochemical analysis of FOXG1 expression in SCLC tissues and the adjacent normal tissues. Scale bar = 50 μm. All data are shown as mean ± SEM. *$P < 0.05$, **$P < 0.01$, ***$P < 0.001$.

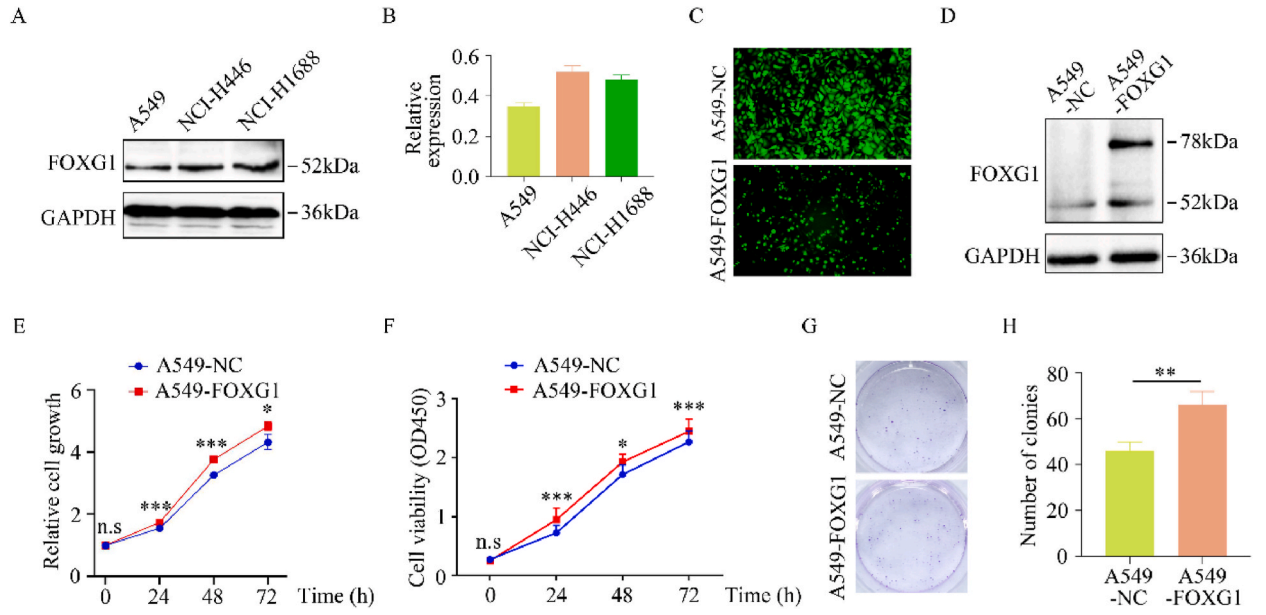

Fig. 2. FOXG1 promoted the proliferation of A549 cells. **A** and **B** Western blotting analysis of FOXG1 expression in lung cancer cell lines. **C** Representative images of the cell line with stably overexpressed FOXG1 (A549-FOXG1) and the control cell line (A549-NC). Scale bar = 100 μm. **D** Western blotting analysis validating FOXG1 overexpression in A549 cells. **E** MTT assay was adopted to estimate cell proliferation ability. **F** Cell Counting Kit-8 assay was used to detect cell viability. **G** and **H** Colony formation assays to assess cell proliferation. All data are shown as mean ± SEM. *P < 0.05, **P < 0.01, ***P < 0.001.

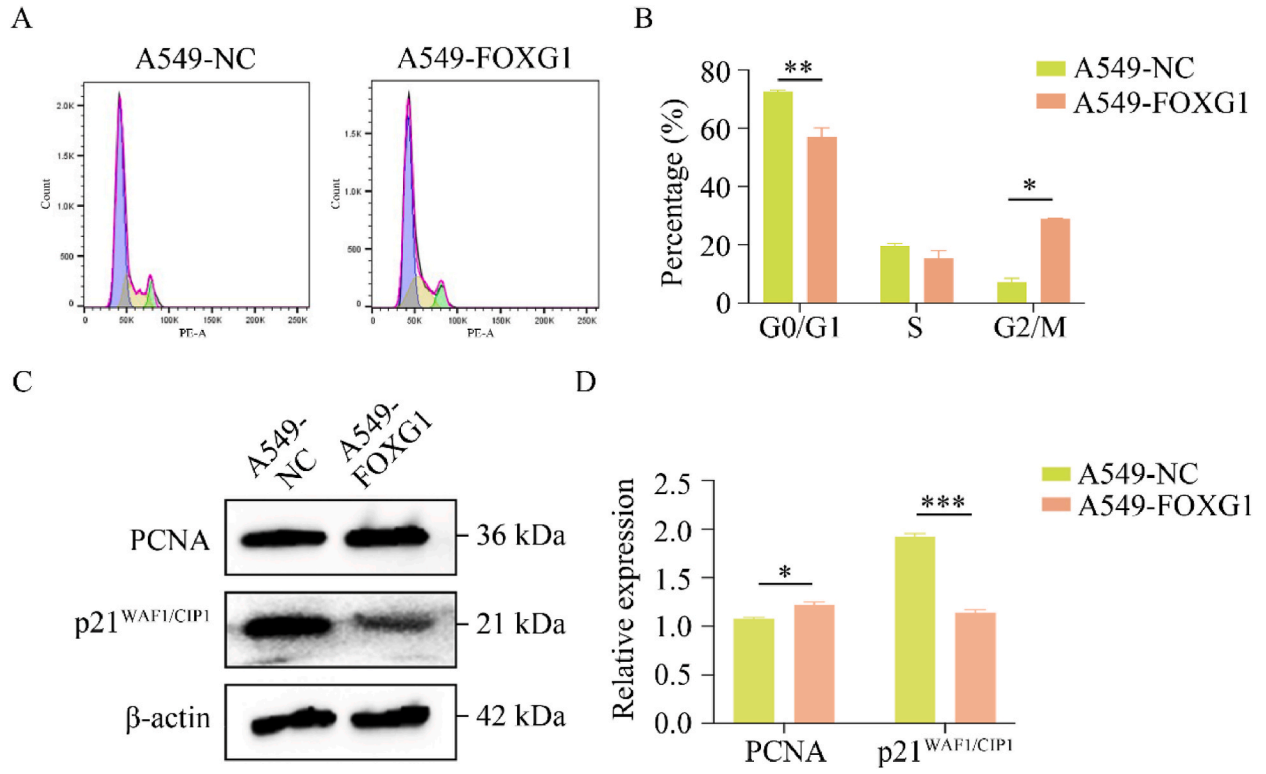

Fig. 3. FOXG1 induced the cell cycle progress of A549 cells. **A** Cell cycle distribution was examined using flow cytometry. **B** The distribution ratio of G0/G1, S, and G2/M of panel A was determined. **C** and **D** Western blotting analysis of PCNA and p21WAF1/CIP1 expression. All data are shown as mean ± SEM. *P < 0.05, **P < 0.01, ***P < 0.001.

We next assessed the effect of FOXG1 on apoptosis. Flow cytometry analysis showed that FOXG1 overexpression inhibited the percentage of early apoptotic A549 cells (Fig. 4A and B). Given the important role of the PI3K pathway in regulating cell survival, PI3K pathway-related proteins were assessed using western blotting to further determine the molecular mechanism mediating the apoptotic effect of FOXG1. The results showed that FOXG1 overexpression substantially increased Akt and mTOR phosphorylation. The PTEN, p53, and Bax expression levels were significantly downregulated in A549-FOXG1 cells compared with the control (Fig. 4C, D, and Fig. S4). These data suggested that FOXG1 could depress apoptosis and activate the PI3K pathway in A549 lung cancer cells.

3.4. *FOXG1 expression promotes the growth of lung cancer in vivo*

We further investigated the carcinogenic effects of FOXG1 *in vivo*. Animal experiments showed that, after planting for 31 days, FOXG1 overexpression significantly promoted tumor growth and increased tumor weight when compared with those in control mice planted with A549-NC (Fig. 5A–C). Western blot analysis verified the successful overexpression of FOXG1 and that FOXG1 could promote PCNA expression in tumor tissues (Fig. 5D–F, and Figs. S5 and 6).

4. Discussion

In this study, we found that the FOXG1 expression level was higher in lung cancer tissues than in normal tissues. Functionally, we

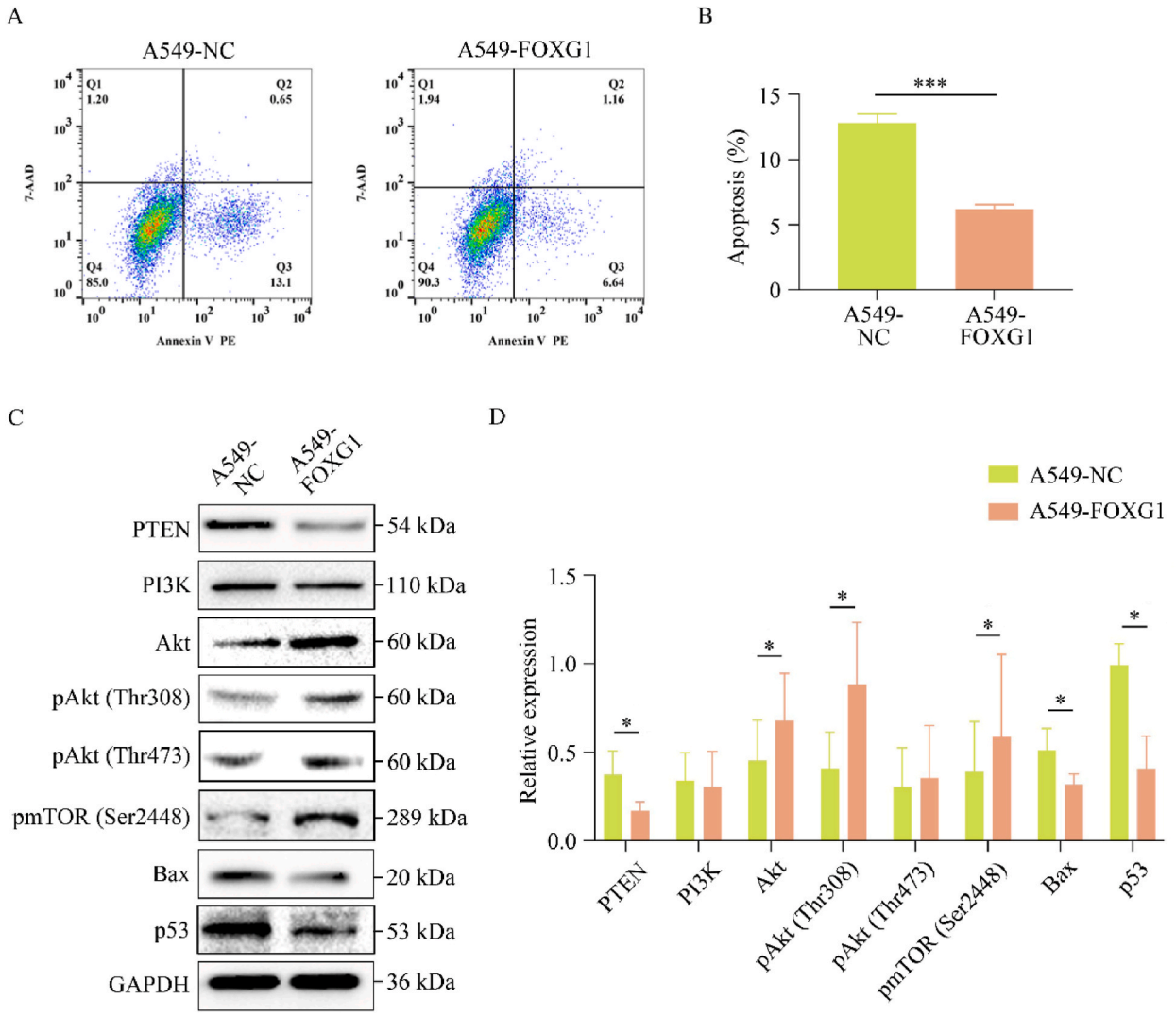

Fig. 4. FOXG1 inhibited the apoptosis of A549 cell. **A** and **B** Cell apoptosis was assessed using flow cytometry. **C** and **D** Western blotting analysis of PTEN, PI3K, Akt, pAkt (Thr308), pAkt (Thr473), pmTOR (Ser2448), Bax, and p53 expression levels. All data are shown as mean ± SEM. *P < 0.05, **P < 0.01, ***P < 0.001.

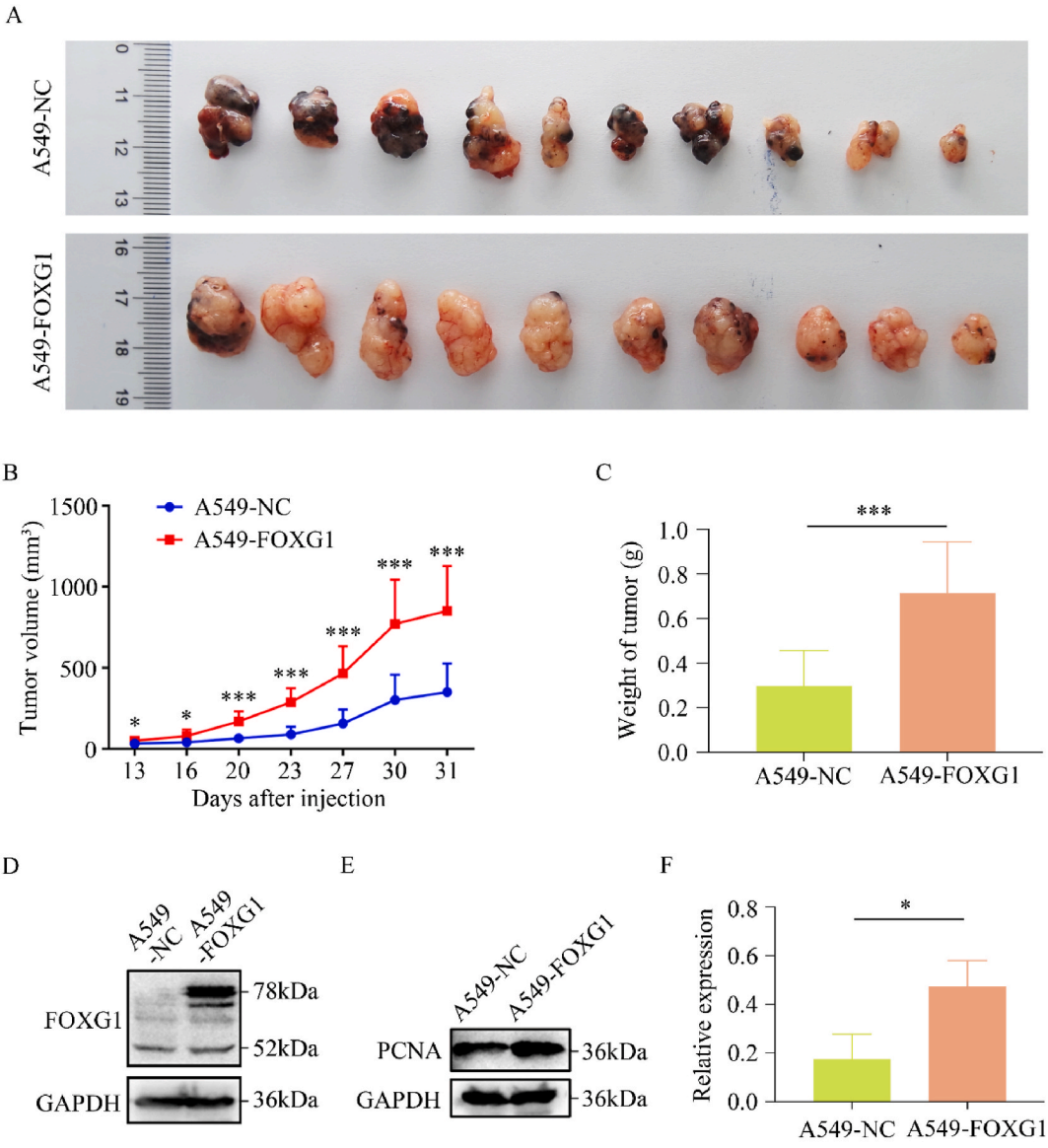

Fig. 5. FOXG1 promoted tumor growth *in vivo*. **A** Representative image of the tumors after planting for 31 days. **B** and **C** Statistical analysis of tumor volume and weight. **D** Western blotting analysis validating FOXG1 overexpression in the tumor tissues. **E** and **F** Western blotting analysis of PCNA expression in the tumor tissues. All data are shown as mean ± SEM. *P < 0.05, ***P < 0.001.

demonstrated that FOXG1 expression strongly promoted lung cancer cell proliferation and inhibited cell apoptosis *in vitro*. Furthermore, *in vivo* experiments confirmed that FOXG1 enhanced tumor formation.

Previous reports of FOXG1 have focused on breast cancer, ovarian cancer, glioma, and other cancers, but only less attention has been paid to the role of FOXG1 in lung cancer. Here, we analyzed the FOXG1 expression level and its prognostic value in lung cancer through bioinformatics analysis. TCGA database analysis showed that FOXG1 expression was significantly higher than that in normal lung tissues in both LUAD and LUSC, and the FOXG1 expression level was related to the prognosis of patients in terms of overall survival. Owing to the limited cases of SCLC in the TCGA database, the Oncomine database was used to analyze the expression level of FOXG1 in SCLC and normal tissues. In two datasets and 38 samples, FOXG1 was overexpressed in SCLC, and the difference was significant. Furthermore, we collected clinical cases of SCLC and performed immunohistochemical experiments, and the results were consistent with those of the bioinformatics analysis.

FOXG1 is a transcriptional repressor with extensive proliferating potential, which is crucial for the progression of many human malignancies. In this study, we found that FOXG1 overexpression significantly promoted A549 cell proliferation by inhibiting apoptosis and promoting the cell cycle. Cell cycle and cell apoptosis are more likely the reasons for altered cell proliferation. First, we inspected the effect of FOXG1 on the lung cancer cell cycle. Consistent with the findings of previous studies, enforced FOXG1

expression inhibited p21WAF1/CIP1 (a negative cell cycle regulator) expression and increased the number of cells in both S and G2/M phases. Thus far, the study of FOXG1 expression in cell apoptosis has been rarely conducted. Previous studies have shown that FOXG1 affects apoptosis through the caspase pathway in glioma and nasopharyngeal carcinoma [18]. The PI3K pathway mediates several cellular functions such as proliferation, migration, and differentiation in various types of cells. Excessive activation of the PI3K pathway usually leads to uncontrolled cell growth. Previous studies mainly focused on the regulation of FOXG1 through PI3K signaling. FOXG1 functions as Smad associates in p21WAF1/CIP1 stimulation, postulating an interrelationship between the TGF-β/Smad and PI3K/Akt pathways and implicating FOXG1 proteins as signal transducers [19]. In our study, we found that FOXG1 overexpression could inhibit early apoptosis and activate the PI3K pathway in A549 lung cancer cells. FOXG1 significantly inhibited PTEN expression and induced Akt, mTOR phospho-activation. Thus, additional in-depth studies are necessary to elucidate the feedback loop regulation between the PI3K pathway and FOXG1 expression. Additionally, the protein expression levels of several apoptotic proteins were assessed. Bax and p53, as pro-apoptotic proteins, showed lower expression levels after inducing FOXG1 overexpression, which further provided evidence for the anti-apoptotic function of FOXG1 in lung cancer cells. Therefore, these findings indicated that the effects of FOXG1 on cell proliferation might be the result of multiple cellular events such as cell apoptosis and cell cycle. Cell apoptosis was more likely the major reason for the altered proliferation of lung cancer cells. Further studies are required to dissect the detailed roles of FOXG1 in promoting tumorigenesis.

In conclusion, FOXG1 shows upregulated expression and plays an oncogenic role in lung cancer. FOXG1 overexpression induces lung cancer cell proliferation and suppresses apoptosis, possibly by activating the PI3K/Akt pathway. Our research findings might provide novel insights into the study of the molecular mechanism of lung cancer.

Funding

This study was funded by the National Natural Science Foundation of China (No.81660465), the Applied Basic Research Program of YunNan Province (No.2014FD045), the Education Department Scientific Research Project of YunNan Province (No.2019Y0267), and the Xingdian Talent Support Program (XDYC-QNRC-2022-0286).

Author contribution statement

Zhenjin Li: Conceived and designed the experiments; Contributed reagents, materials, analysis tools or data.
Mingming Lai: Conceived and designed the experiments; Wrote the paper.
Yuqing Wang: Performed the experiments; Analyzed and interpreted the data; Wrote the paper.
Genyuan Pu; Huijie Jiang: Performed the experiments.
Yan Chen; Caiting Yang; Yongxin Liu; Performed the experiments; Analyzed and interpreted data.
Xiaoting Zhang; Contributed reagents, materials, analysis tools or data.

Data availability statement

Data will be made available on request.

Ethics approval

This study was approved by the Ethics Committee of Dali University (approval no. MECDU-201711-27).

Consent to participate

Informed consent was obtained from all individual participants included in the study.

Declaration of competing interest

The authors declare that they have no known competing financial interests or personal relationships that could have appeared to influence the work reported in this paper.

Acknowledgments

The authors acknowledge Dr. Tao Yang for assistance. We thank TCGA for providing high quality data for public analysis. We thank all the members of the Lai lab and the Department of Pathology, Affiliated Hospital of Dali University for discussion and technical assistance.

Appendix A. Supplementary data

Supplementary data to this article can be found online at https://doi.org/10.1016/j.heliyon.2023.e19540.

References

[1] F. Bray, J. Ferlay, I. Soerjomataram, R.L. Siegel, L.A. Torre, A. Jemal, Global cancer statistics 2018: GLOBOCAN estimates of incidence and mortality worldwide for 36 cancers in 185 countries, Ca - Cancer J. Clin. 68 (6) (2018) 394–424.

[2] M.L. Golson, K.H. Kaestner, Fox transcription factors: from development to disease, Development 143 (24) (2016) 4558–4570.

[3] W. Tao, E. Lai, Telencephalon-restricted expression of BF-1, a new member of the HNF-3/fork head gene family, in the developing rat brain, Neuron 8 (5) (1992) 957–966.

[4] C. Hanashima, S.C. Li, L.J. Shen, E.S. Lai, G. Fishell, Foxg1 suppresses early cortical cell fate, Science 303 (5654) (2004) 56–59.

[5] B. Martynoga, H. Morrison, D.J. Price, J.O. Mason, Foxg1 is required for specification of ventral telencephalon and region-specific regulation of dorsal telencephalic precursor proliferation and apoptosis, Dev. Biol. 283 (1) (2005) 113–127.

[6] F. Ariani, G. Hayek, D. Rondinella, R. Artuso, M.A. Mencarelli, A. Spanhol-Rosseto, M. Pollazzon, S. Buoni, O. Spiga, S. Ricciardi, I. Meloni, I. Longo, F. Mari, V. Broccoli, M. Zappella, A. Renieri, FOXG1 is responsible for the congenital variant of Rett syndrome, Am. J. Hum. Genet. 83 (1) (2008) 89–93.

[7] F. Kortum, S. Das, M. Flindt, D.J. Morris-Rosendahl, I. Stefanova, A. Goldstein, D. Horn, E. Klopocki, G. Kluger, P. Martin, A. Rauch, A. Roumer, S. Saitta, L. E. Walsh, D. Wieczorek, G. Uyanik, K. Kutsche, W.B. Dobyns, The core FOXG1 syndrome phenotype consists of postnatal microcephaly, severe mental retardation, absent language, dyskinesia, and corpus callosum hypogenesis, J. Med. Genet. 48 (6) (2011) 396–406.

[8] J.A. Siegenthaler, B.A. Tremper-Wells, M.W. Miller, Foxg1 haploinsufficiency reduces the population of cortical intermediate progenitor cells: effect of increased p21 expression, Cerebr. Cortex 18 (8) (2008) 1865–1875.

[9] F. Verginelli, A. Perin, R. Dali, K.H. Fung, R. Lo, P. Longatti, M.C. Guiot, R.F. Del Maestro, S. Rossi, U. di Porzio, O. Stechishin, S. Weiss, S. Stifani, Transcription factors FOXG1 and Groucho/TLE promote glioblastoma growth, Nat. Commun. 4 (2013) 2956.

[10] A.M. Adesina, Y. Nguyen, P. Guanaratne, J. Pulliam, D. Lopez-Terrada, J. Margolin, M.J.H.P. Finegold, FOXG1 is overexpressed in hepatoblastoma 38 (3) (2007) 400–409.

[11] D.W. Chan, V. Liu, R. To, P.M. Chiu, W. Lee, K.M. Yao, A. Cheung, H.J.B.J.o.C. Ngan, Overexpression of FOXG1 contributes to TGF-β resistance through inhibition of p21WAF1/CIP1 expression in ovarian cancer 101 (8) (2009) 1433–1443.

[12] J.V. Li, C.D. Chien, J.P. Garee, J. Xu, W. Anton, A.T.J.M.E. Riegel, Transcriptional repression of AIB1 by FoxG1 leads to apoptosis in, Breast Cancer Cells (7) (2013) 1113–1127.

[13] H. Xi, Z. He, C. Lv, FOXG1 improves mitochondrial function and promotes the progression of nasopharyngeal carcinoma, Mol. Med. Rep. 24 (3) (2021).

[14] C. Dou, J. Lee, B. Liu, F. Liu, J. Massague, S. Xuan, E. Lai, BF-1 interferes with transforming growth factor beta signaling by associating with Smad partners, Mol. Cell Biol. 20 (17) (2000) 6201–6211.

[15] T. Watanabe, T. Miura, Y. Degawa, Y. Fujita, M. Inoue, M. Kawaguchi, C. Furihata, Comparison of lung cancer cell lines representing four histopathological subtypes with gene expressio n profiling using quantitative real-time PCR, Cancer Cell Int. 10 (2010) 2.

[16] X. Xu, J. Nie, L. Lu, C. Du, F. Meng, D. Song, YAP-TEAD up-regulates IRS2 expression to induce and deteriorate oesophageal cancer, J. Cell Mol. Med. 25 (5) (2021) 2584–2595.

[17] J. Gao, X. Qiu, G. Xi, H. Liu, F. Zhang, T. Lv, Y. Song, Downregulation of GSDMD attenuates tumor proliferation via the intrinsic mitochondrial apoptotic pathway and inhibition of EGFR/Akt signaling and predicts a good prognosis in nonsmall cell lung cancer, Oncol. Rep. 40 (4) (2018) 1971–1984.

[18] J. Chen, X. Wu, Z. Xing, C. Ma, W. Xiong, X. Zhu, X. He, FOXG1 expression is elevated in glioma and inhibits glioma cell apoptosis, J. Cancer 9 (5) (2018) 778–783.

[19] J. Seoane, H.V. Le, L. Shen, S.A. Anderson, J. Massagüí, Integration of Smad and forkhead pathways in the control of neuroepithelial and glioblastoma cell pro liferation, Cell 117 (2) (2004) 211–223. Statements and Declarations.